ORGANIC PROCESS RESEARCH & DEVELOPMENT
OPR&D

pubs.acs.org/OPRD Article

Development of a Scalable Negishi Cross-Coupling Process for the Preparation of 2-Chloro-5-(1-(tetrahydro-2*H*-pyran-2-yl)-1*H*-pyrazol-5-yl)aniline

Candice L. Joe,* Bahar Inankur, James Chadwick, Sha Lou, Jeffrey Nye, Neil A. Strotman, and Albert J. DelMonte

Cite This: https://dx.doi.org/10.1021/acs.oprd.0c00414 Read Online

ACCESS | Metrics & More | Article Recommendations | Supporting Information

ABSTRACT: A scalable synthesis of 2-chloro-5-(1-(tetrahydro-2*H*-pyran-2-yl)-1*H*-pyrazol-5-yl)aniline (**1**), a key intermediate in the synthesis of an immuno-oncology asset, is described. A Negishi cross-coupling between *in situ* generated heteroaryl zinc reagent **4** and 5-bromo-2-chloroaniline (**3**) catalyzed by Pd(Xantphos)Cl_2 enabled the construction of the key aryl−heteroaryl bond. A scalable first-generation process was developed that delivered **1** in multikilogram quantities. Building upon knowledge from the initial process, a more efficient workup and isolation procedure was developed that controlled levels of residual Pd and Zn to consistent levels that were acceptable for downstream processing. The high-yielding optimized process offers streamlined metals remediation, a 30% reduction in the number of unit operations, and a 34% reduction in process mass intensity (PMI) compared to the initial process.

KEYWORDS: *Zinc, Negishi, Pd-catalyzed, metals remediation, pyrazole, hexyllithium*

INTRODUCTION

During the development of an immuno-oncology asset, 2-chloro-5-(1-(tetrahydro-2*H*-pyran-2-yl)-1*H*-pyrazol-5-yl)-aniline (**1**) was identified as a key intermediate in the first step of a convergent synthetic route. A robust chemical process to deliver **1** in multikilogram quantities was required to support downstream process development. While there are many possible approaches to prepare **1**, we identified the aryl−heteroaryl bond as the key disconnection (Figure 1). To achieve this goal, the appropriate protected pyrazole and 2,5-bis-halogenated aniline starting materials were required. We identified 1-(2-tetrahydropyranyl)-1*H*-pyrazole **2** as a competent coupling partner. The tetrahydropyranyl (THP) group is compatible with downstream chemistry and can easily be removed later in the synthesis. Although the potential introduction of added analytical complexity from using the chiral THP protecting group should always be considered, this was not a confounding factor in the preparation of **1**. 5-Bromo-2-chloroaniline **3** was chosen as the electrophile, as it allowed for selective functionalization at the 5-position and provided a handle for subsequent functionalization at the 2-position. Most importantly, both **2** and **3** are readily available commercial starting materials. Herein, we disclose a streamlined and high yielding Negishi[1] cross-coupling process for the preparation of **1**.

C−C BOND FORMING STRATEGIES

Our development work focused on the construction of the key C−C bond using metal-catalyzed cross coupling methods (Scheme 1). Of particular interest was the regioselective palladium-catalyzed direct C−H arylation of pyrazoles reported by Sames and co-workers.[2] Small scale experiments using a 3-fold excess of **2** revealed that the transformation was, indeed, selective for the desired regioisomer, albeit in an 85:15 ratio[3] relative to other mono- and bis-functionalized pyrazole side products (Scheme 1). As we anticipated it could be difficult to purge high levels of these structurally similar side products (*vide infra*) in subsequent steps, we focused efforts on identifying milder conditions to selectively functionalize the 5-position of **2**. In particular, pyrazole **2** is known to undergo selective deprotonation at the 5-position at −78 °C with *n*-butyllithium (*n*-BuLi), followed by trapping with an alkyl electrophile.[4,5] We hypothesized that transmetalation of the heteroaryl lithium of **2** to an appropriate zinc salt would generate a heteroaryl zinc reagent *in situ* that could participate in Negishi cross-coupling with **3** to generate **1**.[6,7] Proof-of-concept experiments suggested that this was the case, with **1** formed selectively and no observable overfunctionalization of the aniline ring (Scheme 1).

HIGH-THROUGHPUT CATALYST SCREENING

After achieving proof-of-concept for the Negishi coupling, a high-throughput catalyst screen was initiated (24 μmol scale). Follow-up experiments revealed that deprotonation of **2** with *n*-BuLi and transmetalation to $ZnCl_2$ occurred at −10 °C,

Special Issue: Celebrating Women in Process Chemistry

Received: September 18, 2020

https://dx.doi.org/10.1021/acs.oprd.0c00414
Org. Process Res. Dev. XXXX, XXX, XXX−XXX

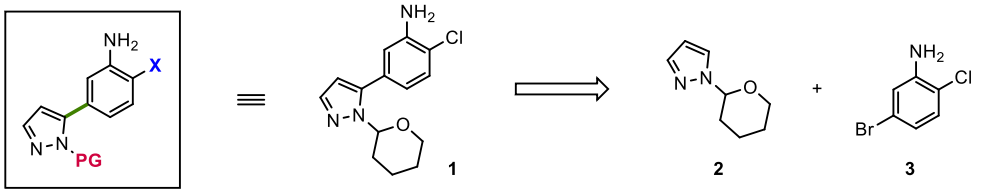

Figure 1. Retrosynthetic analysis of **1**.

Scheme 1. Cross-coupling Approaches to 1

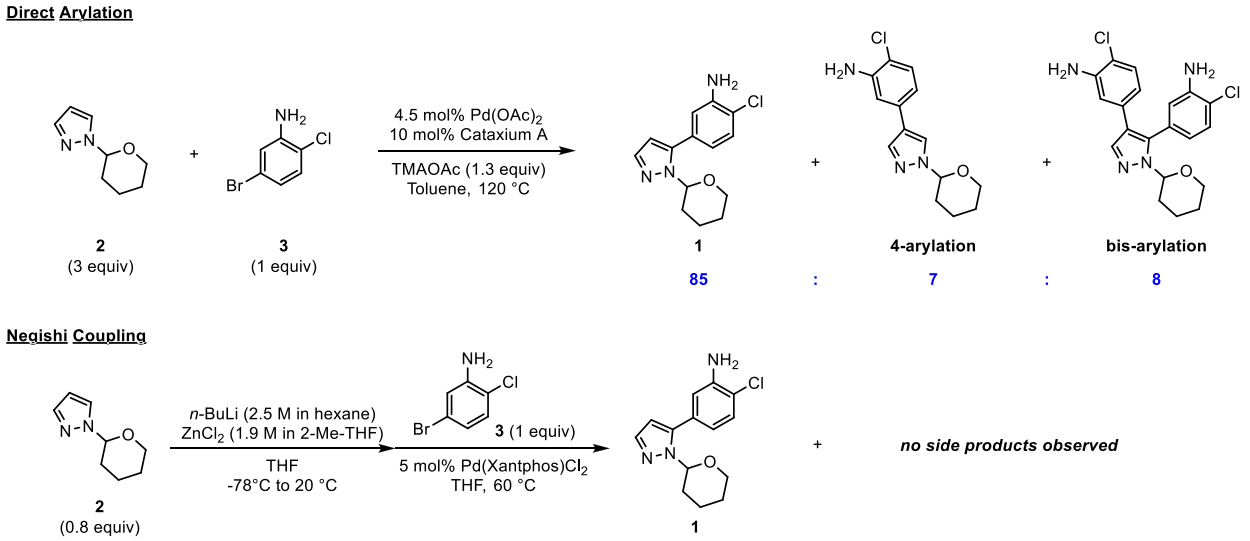

Table 1. Selected Ligand Screening Results from HTE Screen

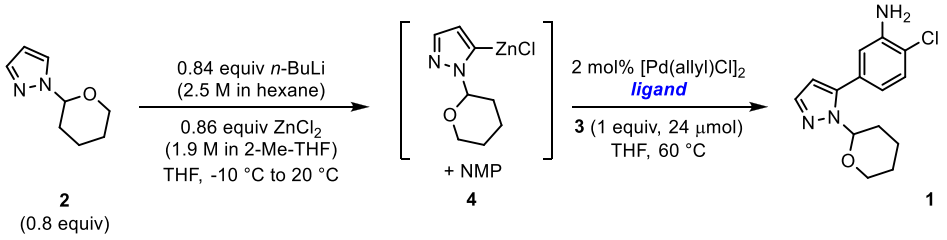

Entry	Ligand[a]	1 (AP)[b]
1	PPh_3	42
2	$PCy_3{\cdot}HBF_4$	34
3	$P(t\text{-}Bu)_3{\cdot}HBF_4$	81
4	X-Phos	87
5	S-Phos	67
6	RuPhos	74
7	Cy-JohnPhos	62
8	Xantphos	84
9	Cy-Xantphos	12
10	DPEPhos	77
11	DCEPhos	79
12	DPPF	63
13	DPPE	64

[a]The ligand/metal (L/M) ratio for monodentate phosphine ligands was 2.2:1, and the L/M ratio for bidentate ligands was 1.1:1. [b]Area percent (AP) was determined by UPLC-MS.

which obviates the need to achieve cryogenic temperatures on scale. Using this modified procedure, heteroaryl zinc reagent **4** was generated in a single batch that exists as a slurry upon warming to 20 °C. The addition of 20 vol % *N*-Methyl-2-pyrrolidone (NMP) was necessary to fully dissolve heteroaryl zinc **4**, thus facilitating uniform dosing into each screening vial.[8] Screening 36 ligands with 2 mol % $[Pd(allyl)Cl]_2$ revealed a number of promising ligands with selected results shown in Table 1.[9] The best ligands included $P(t\text{-}Bu)_3{\cdot}HBF_4$ (entry 3), X-Phos (entry 4), and Xantphos (entry 8), all of

https://dx.doi.org/10.1021/acs.oprd.0c00414
Org. Process Res. Dev. XXXX, XXX, XXX−XXX

Scheme 2. Comparison at 1.5 mol % Catalyst Loading

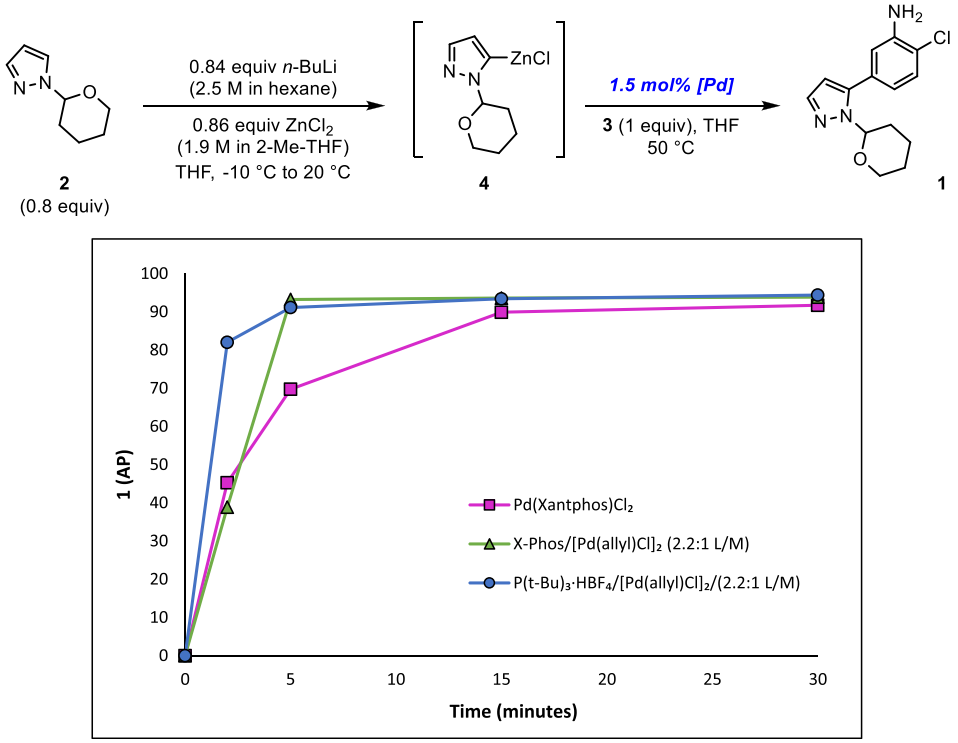

Scheme 3. Initial Negishi Process To Generate 1

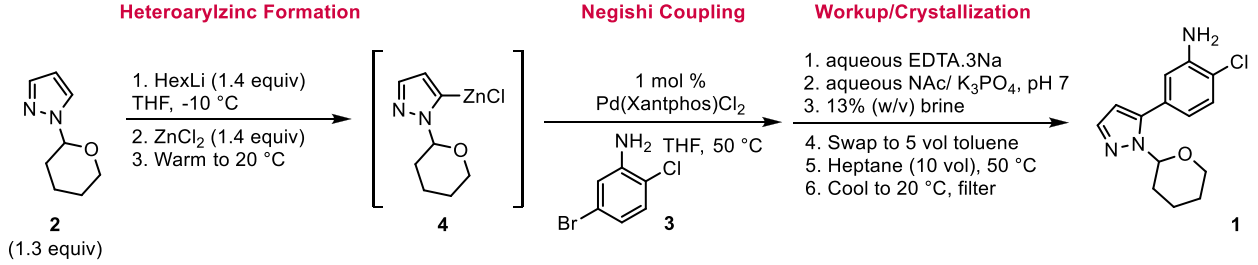

which provided Negishi product **1** in >80 area percent (AP) with the remainder of the mass balance as residual starting materials.

A further evaluation of catalyst activity was undertaken on 650 μmol scale using P(*t*-Bu)$_3$·HBF$_4$/[Pd(allyl)Cl]$_2$ (2.2:1 L/M ratio), X-Phos/[Pd(allyl)Cl]$_2$ (2.2:1 L/M ratio), and Pd(Xantphos)Cl$_2$ at 50 °C. All catalyst systems exhibited fast kinetics in the Negishi coupling to form **1** at 50 °C, with all reactions reaching completion (>95 AP **1**) within 30 min (Scheme 2). Despite exhibiting the slowest kinetics of the three catalyst combinations, pre-complexed Pd(Xantphos)Cl$_2$ was pursued to minimize the number of required unit operations during scale-up. In particular, the use of this catalyst avoids a metal/ligand pre-complexation step that would require a separate catalyst preparation vessel followed by an inert transfer to the *in situ* generated solution of **4**.

The reaction is a two-step process: *in situ* formation of heteroaryl zinc **4** followed by Negishi coupling with **3**. In the context of high-throughput screening, it was more practical to generate **4** in a single solvent system, THF/hexane/2-Me-THF (where hexane and 2-Me-THF were introduced by *n*-BuLi and ZnCl$_2$, respectively), to compare catalysts and ligands. This avoids any inconsistencies that could originate during the zincate formation and manifest in the Negishi screening results. The use of 2-Me-THF during the formation of heteroaryl zinc **4** would obviate the need for a ternary reaction solvent mixture. While 2-Me-THF and THF both provided a high AP of **1** in a similarly fast time frame, the heteroaryl lithium intermediate was a thick slurry in 2-Me-THF that made agitation challenging. By contrast, the heteroaryl lithium slurry is thinner and more easily suspended in THF, making it a better choice of reaction solvent for scale up purposes with overhead stirring.

INITIAL PROCESS

With the palladium catalyst selected, we began to develop an enabling process to deliver kilogram quantities of **1** to support downstream process development (Scheme 3). Initial catalyst screening was performed using **2** as the limiting reagent. However, we quickly realized the benefits of making **3** the limiting agent (Scheme 3) due to the more efficient purge of residual pyrazole **2** compared to the rejection of **3** during the crystallization (*vide infra*).[10]

Process safety and environmental concerns led us to replace *n*-BuLi with *n*-hexyllithium (HexLi) for scale up purposes,[11] with the deprotonation of pyrazole **2** also proceeding smoothly

https://dx.doi.org/10.1021/acs.oprd.0c00414
Org. Process Res. Dev. XXXX, XXX, XXX−XXX

at −10 °C with HexLi. The heteroaryl lithium intermediate was found to be a slurry, and the deprotonation event exothermic with an adiabatic temperature rise of 48 °C.[12] A 30 min slow addition of HexLi to a −10 °C solution of pyrazole **2** in THF could control the exotherm. In doing so, the internal temperature was never greater than 5 °C and *in situ* FTIR spectroscopy confirmed that the consumption of pyrazole **2** is essentially addition-controlled. The addition of the $ZnCl_2$ solution to the heteroaryl lithium slurry was also exothermic, exhibiting an adiabatic temperature rise of 35 °C. Slow addition of the $ZnCl_2$ solution over 30 min mitigated the safety risk of this exotherm and generated heteroaryl zinc species **4** safely.

The Negishi coupling reached full conversion within 1 h using 1.4 equiv of $ZnCl_2$ (1.9 M solution in 2-Me-THF). Full conversion to **1** was also observed within 1 h when substoichiometric amounts of the $ZnCl_2$ solution (0.7 equiv) were used, albeit with slightly slower reaction kinetics (Figure 2).[7i,13] Solid $ZnCl_2$ and $ZnBr_2$ were also suitable Zn precursors

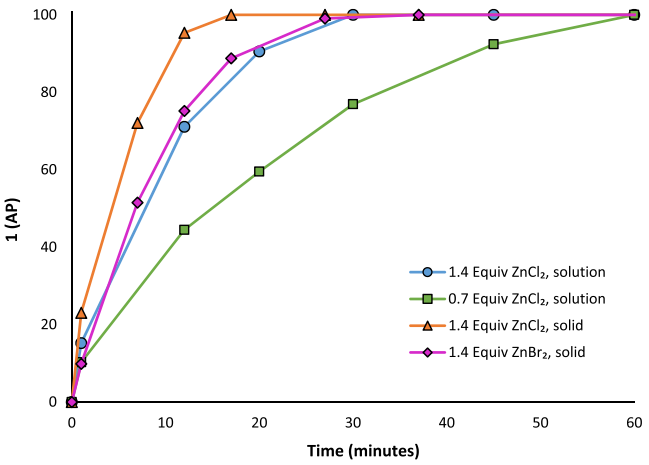

Figure 2. Effect of ZnX_2 source and stoichiometry on reaction kinetics.

to access the heteroaryl zinc intermediate, with the Negishi coupling reaching full conversion in a similar time frame to the reaction using the $ZnCl_2$ solution (Figure 2). The $ZnCl_2$ solution in 2-Me-THF solution was preferred for scale up purposes due to robustness concerns around suspending solid zinc salts in the reactor early in the transmetalation process and the potential challenges of reliably sourcing high quality anhydrous ZnX_2 in bulk quantities. The 2-Me-THF solution of $ZnCl_2$ has been consistently sourced with a KF < 1100 ppm, thus mitigating the risk of heteroaryl lithium quenching due to the presence of water. Since excess zinc was easily purged during the workup (*vide infra*), the $ZnCl_2$ charge was maintained at 1.4 equiv to ensure process robustness.

Once the $ZnCl_2$ solution charge was complete, the slurry of *in situ* generated **4** was warmed to 20 °C. Aniline **3** and $Pd(Xantphos)Cl_2$ were charged to the reactor containing the heteroaryl zinc slurry with extra care taken to exclude oxygen. The Negishi coupling began upon heating the contents of the reactor to 50 °C and aging for 4 h, which consistently delivered **1** in >98% in-process yield.

The main side product observed at the end of reaction is **6**, which arises from transmetalation of HexLi to $ZnCl_2$ and coupling of the corresponding hexylzinc species **5** with **3** under the Negishi coupling conditions (Scheme 4). Analysis of the end-of-reaction HPLC purity reveals that hexyl-coupled impurity **6** is typically formed in <1 AP. While lowering the equivalents of HexLi and $ZnCl_2$ relative to **2** suppressed the formation of **6**, we found that a small overcharge of these reagents in the heteroaryl zinc formation step increased robustness by accounting for slight deviations in the potency of the HexLi and $ZnCl_2$ solutions.[14] Moreover, **6** is efficiently purged under our crystallization conditions. Notably, no side products arising from overfunctionalization or dehalogenation of the aniline ring were detected under the Negishi reaction conditions. The THP protecting group also remained intact throughout the process, which further highlights the mild reaction and workup conditions (*vide infra*).

An appropriate metals remediation strategy is crucial for the development of metal-catalyzed cross-coupling processes; in the case of a Negishi coupling, metals removal must be particularly robust, requiring the removal of both stoichiometric quantities of Zn and catalytic amounts of Pd.[15] In particular, high levels of Zn and Pd would challenge the crystallization and potentially impact downstream transformations and, ultimately, API quality. For the development of our initial fit-for-purpose process, remediation of the two metals was done in a stepwise fashion. Ideally, a Zn remediation method would (1) quench the excess aryl zinc reagent by protonolysis, (2) complex liberated zinc, and (3) partition the Zn complex to the aqueous layer. The end-of-reaction stream was washed with an aqueous solution of ethylenediaminetetraacetic acid trisodium (EDTA·3Na) and efficiently partitioned >98% of Zn to the aqueous layer, with only 0.4 ppm remaining in the product-rich organic phase (Table 2).[7d] Unfortunately, the EDTA·3Na wash was not an efficient Pd scavenger, with no reduction in Pd levels observed in the organic phase. A second wash with pH = 7 aqueous *N*-

Table 2. Metals Remediation in the Initial Process[a]

Analyte	End-of-reaction stream	EDTA·3Na Wash	NAc Wash, pH = 7
Zn (ppm)	27,886	0.4	0.4
Pd (ppm)	325	338	103

[a]Levels of residual metals in the product-rich organic phase were determined by X-ray Fluorescence Spectroscopy (XRF).

Scheme 4. Formation of Hexyl-Coupled Impurity 6

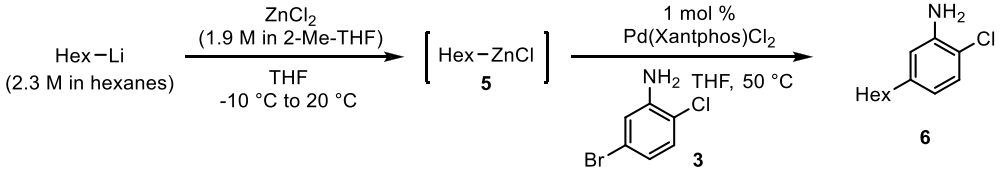

https://dx.doi.org/10.1021/acs.oprd.0c00414
Org. Process Res. Dev. XXXX, XXX, XXX−XXX

acetylcysteine (NAc) reduced the Pd levels in the organic layer by approximately 70%. An additional 13% brine wash removed residual inorganics from the organic phase prior to isolation of **1**.

Cross-coupled product **1** exhibited high solubility (>50 mg/mL) in the majority of common solvents (Table 3). For isolation, a swap to a solvent with a higher boiling point than the ternary reaction solvent mixture (THF/2-Me-THF/hexane) was desired to derisk variations in the ternary solvent ratios from batch to batch depending on solvent losses during the reaction and workup. A solvent swap to a higher boiling solvent at a fixed volume post-workup would provide a platform for a controlled crystallization without variability arising from residual reaction solvents. We identified three high boiling solvents where **1** exhibits lower solubility than the reaction solvents: isopropanol (*i*-PrOH), cyclopentyl methyl ether (CPME), and toluene. Water and heptane were the only suitable anti-solvents identified based on low solubility of **1** (<5 mg/mL). Based on this solubility data, a number of solvent/anti-solvent combinations[16] were screened to identify a system capable of isolating **1** as a crystalline solid while purging **2** and any residual **3**. A key criteria for solvent/anti-solvent selection was a >30 mg/mL solubility difference between **1** and **3**. We ultimately pursued a toluene/heptane crystallization for our enabling process due to its better purge of the aniline **3** in the event of incomplete conversion.

In the lab, **1** was consistently isolated in up to 80% yield (>99.5 wt % and >99.4 LCAP purity) with acceptable levels of residual metals (773 ppm Pd, 0.9 ppm Zn) on 10−50 g scale. The scalability of this process was then demonstrated by the successful delivery of three 2-kg batches of **1** with similar yields and quality as observed on laboratory scale.

Table 3. Selected Solubility Data for 1 and 3 at 20 °C

Solvent	Boiling point	Product **1** (mg/mL)	Aniline **3** (mg/mL)
THF	66 °C	410	1301
2-Me-THF	80 °C	154	1145
i-PrOH	83 °C	36	605
CPME	106 °C	128	659
Toluene	111 °C	95	896
Water	100 °C	0.003	0.03
Heptane	98 °C	1	58
33% Toluene/ 66% Heptane	100 °C	6	308
33% CPME/ 66% Heptane	98 °C	9	462
33% *i*-PrOH/66% Water	82 °C	3	10

[a]Solvent ratios are reported in v/v.

OPTIMIZED PROCESS

The successful scale up of the initial process allowed us to identify various areas for improvement. For example, the workup required high kg/kg loadings of EDTA·3Na due to the limited solubility of EDTA·3Na in water. This led to large V_{min}/V_{max} swings of the process stream during extraction. Moreover, the aqueous NAc wash proved to be inconsistent on scale with respect to Pd remediation. The requirement for three aqueous washes for Pd and Zn remediation also resulted in longer-than-ideal processing times and higher PMI due to the waste stream generation. We sought to develop an improved process that addressed these drawbacks with a particular focus on streamlining the workup (Scheme 5).

A more efficient metals remediation strategy would remove Pd and Zn in a single workup step. To evaluate this possibility, a survey of potential scavengers was carried out on the end-of-reaction stream (Table 4). Quenching the end-of-reaction stream with 10% aqueous NH_4OAc resulted in a clean phase split but incomplete removal of Zn and Pd. While the efficient removal of Pd and Zn was observed with a single pH 8 *N*-acetylcysteine wash, this was accompanied by an emulsion that made phase separation difficult. An aqueous ethylene diamine wash efficiently lowered the Zn levels in the organic phase to levels similar to that of EDTA·3Na.[7c,17] As an added benefit, 3.2 kg/kg EDTA·3Na in 12 volumes of water was required for efficient Zn remediation, whereas 1.6 kg/kg ethylene diamine in 8 volumes of water was sufficient to lower Pd and Zn levels. For this reason, the aqueous ethylene diamine wash was more attractive from an efficiency and PMI perspective.

Table 4. Scavenger Screen for Pd and Zn Remediation[18]

Scavenger	Zn, ppm	Pd, ppm	Notes
No wash	27,886	325	
10% w/v $NH_4OAc_{(aq)}$	4653	401	Clean phase split
$EDTA{\cdot}3Na_{(aq)}$	0.3	392	Clean phase split
Ethylene $diamine_{(aq)}$	1.4	218	Clean phase split
$NAc_{(aq)}$, pH = 8	Not detected	104	Emulsion
SiliaMetS Thiol	12667	348	Requires filtration

[a]Levels of residual metals in the product-rich organic phase were determined by XRF.

Quenching the reaction with an aqueous ethylene diamine solution resulted in an adiabatic temperature rise of 15 °C. While the exotherm was easily controlled by the slow addition of the ethylene diamine quench solution over 90 min, some solids formed in early stages of the addition. To avoid potential hang-up of solids in the reactor, a reverse quench, whereby the end-of-reaction stream was charged to the aqueous ethylene diamine solution, was implemented for subsequent campaigns.

Scheme 5. Optimized Negishi Process To Generate 1

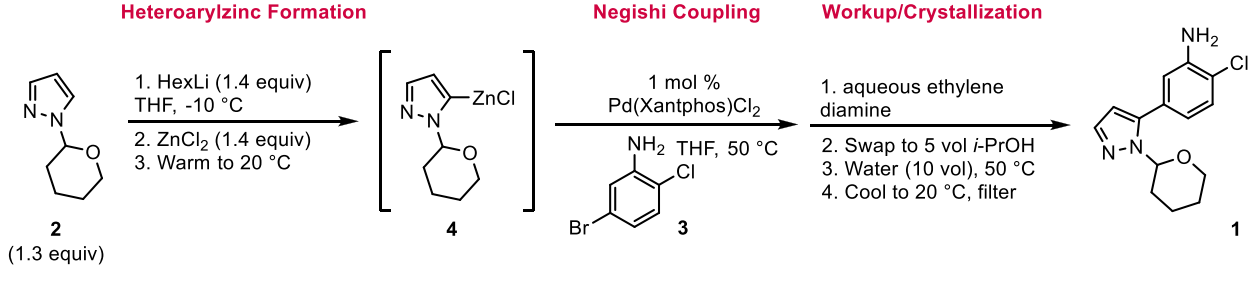

https://dx.doi.org/10.1021/acs.oprd.0c00414
Org. Process Res. Dev. XXXX, XXX, XXX−XXX

With a streamlined workup procedure in hand, the effect on the crystallization and residual metals levels in the isolated solids was further investigated (Table 5). The toluene/heptane crystallization gave **1** in comparable yield and purity to the initial process; however, residual Pd and Zn levels in isolated material were significantly higher. Based on the solubility data for **1** (Table 3), we expected that an *i*-PrOH/water crystallization would provide **1** with low product losses to the mother liquor and is differentiated in its solvent polarity from the toluene/heptane system. Performing an *i*-PrOH/water crystallization after the aqueous ethylene diamine wash provided **1** in high yield and quality and, most importantly, with low levels of residual metals. Additionally, the toluene/heptane and *i*-PrOH/water crystallization conditions provided the same crystal form of **1**. Analysis of the mother liquor and subsequent washes revealed that *i*-PrOH/water was capable of further purging trace metals post-workup whereas toluene/heptane was not. Drying the wet cake overnight under vacuum at 50 °C ensured that residual solvents and ethylene diamine were removed. The control of residual ethylene diamine is an important quality attribute in the dry cake of **1**, as it can act as a catalyst poison in subsequent metal-catalyzed steps. The isolation procedure provided consistent control over the ethylene diamine levels to <0.05 wt % in the dry cake.

Table 5. Lab Scale Comparison of Crystallization Conditions on Quality of Isolated 1

Solvent System	Yield	Purity (LCAP)	Pd, ppm	Zn, ppm
Toluene/heptane	82%	99.4	1665	205
i-PrOH/water	88%	99.6	171	5

The optimized process was executed on 300-g scale, delivering **1** in 88% yield and 99.6 LCAP purity. Importantly, the combination of the ethylene diamine workup and *i*-PrOH/water crystallization efficiently purged metals to an acceptable level with only 426 ppm Pd and 0.8 ppm Zn remaining in the isolated solids. These levels of Pd and Zn had no impact on the subsequent steps or the purity of our drug candidate.

CONCLUSIONS

A scalable and robust Negishi coupling process was developed that delivers **1** in consistent yield and quality that was acceptable for downstream processing. This was enabled by a variety of workflows: high-throughput experimentation to identify the appropriate catalyst, solubility screening to find an optimal crystallization solvent combination, and metal scavenger screening to streamline the workup procedure. Compared to the enabling process, the optimized process offers a streamlined metals remediation, a 30% reduction in the number of unit operations, and a 34% reduction in process mass intensity[19] (PMI, Table 6). This was accomplished by using an aqueous ethylene diamine wash to remove residual Zn and Pd and implementing an *i*-PrOH/water crystallization that is capable of further purging trace metal impurities post-workup.

Table 6. Comparison of the Initial and Optimized Negishi Processes

	Initial Process	Optimized Process	Improvement
Workup	3 extractions	1 extraction	Streamlined metals remediation
Unit Operations	7	5	30% reduction
Purity (LCAP)	99.4	99.6	Good quality control
Potency (wt%)	99.4%	99.7%	Good quality control
PMI	79	52	34% reduction

EXPERIMENTAL SECTION

All operations were performed under a nitrogen atmosphere. Starting materials, reagents, and solvents were used as-received from commercial vendors. Standard benchtop techniques were employed for handling air- and moisture-sensitive reagents. Hexyllithium (2.3 M in hexane) and $ZnCl_2$ (1.9 M in 2-Me-THF) were purchased from Sigma-Aldrich. UPLCMS analysis was performed using a Waters Acquity BEH Shield RP-18 column (1.7 μm, 2.1 mm × 50 mm) with detection by UV at 220 nm and low resolution mass spectrometry detection (positive ion mode) with a Shimadzu LCMS-2020 mass spectrometer. HPLC analysis was performed using a Supelco Ascentis Express C-18 column (2.7 μm, 4.6 mm × 50 mm) with UV detection at 220 nm. High-resolution mass spectrometry (HRMS) was performed on an Agilent 6230B TOF mass spectrometer. Data are presented as follows: chemical shift (ppm), multiplicity (s = singlet, d = doublet, t = triplet, m = multiplet, br = broad), coupling constant *J* (Hz), and integration. Trace metals analysis was carried out using two techniques: (1) X-ray fluorescence spectroscopy (XRF) on a Malvern Panalytical Epsilon 1 spectrometer and (2) Inductively coupled plasma atomic emission spectroscopy (ICP-OES) using a ThermoFisher iCap 7400 spectrometer.

2-Chloro-5-(1-(tetrahydro-2*H*-pyran-2-yl)-1*H*-pyrazol-5-yl)aniline (1). *Initial Process.* A solution of 1-(tetrahydro-2*H*-pyran-2-yl)-1*H*-pyrazole **2** (479 g, 3.1 mol, 1.3 equiv) in THF (4 L, 8 L/kg) was inerted via subsurface N_2 sparging and cooled to −10 °C. A solution of hexyllithium in hexane (1.4 L, 2.3 M, 3.2 mol, 1.35 equiv) was charged over 30 min such that the internal temperature remained below 5 °C. After aging the slurry for 20 min, a solution of $ZnCl_2$ in 2-methyltetrahydrofuran (1.7 L, 1.9 M, 3.4 mol, 1.4 equiv) was added portionwise such that the internal temperature remained below 5 °C. The slurry was warmed to 20 °C and inerted via subsurface N_2 sparging. 5-Bromo-2-chloroaniline **3** (500 g, 2.4 mol, 1.0 equiv), dichloro[9,9-dimethyl-4,5-bis(diphenylphosphino)xanthene]palladium(II) (18.5 g, 24 mmol, 0.01 equiv), and THF (800 mL, 1.6 L/kg) were charged to the reactor. The reaction mixture was heated to 50 °C for 4 h and cooled to 20 °C once the reaction was judged to be complete by HPLC analysis.

A solution of ethylenediaminetetraacetic acid trisodium (1.6 kg, 4.3 mol, 1.8 equiv) and water (6 L, 12 L/kg) was added to the vessel. The mixture was stirred for 4 h, and the aqueous layer was removed. The organic layer was washed with a solution of *N*-acetyl-L-cysteine (625 g, 3.8 mol, 1.6 equiv), potassium phosphate tribasic (675 g, 3.1 mol, 1.4 equiv), and water (3 L, 6 L/kg) and aged at 20 °C for 14 h. The aqueous layer was removed, and the organic layer was washed with 13% brine (2.5 L, 5 mL/g). After the aqueous layer was discarded, the organic layer was concentrated to 2.5 L (5 L/kg) followed by constant-volume distillation and solvent exchange to toluene. The temperature of the batch was adjusted to 45 °C followed by the addition of heptane (1.5 L, 3 L/kg) and aging at 45 °C for 1 h to facilitate formation of a seed bed.

https://dx.doi.org/10.1021/acs.oprd.0c00414
Org. Process Res. Dev. XXXX, XXX, XXX−XXX

Heptane (3.5 L, 7 L/kg) was charged at 45 °C, and the batch was aged at this temperature after the addition was complete. The batch was cooled to 20 °C over 1 h and aged for an additional 8 h. Filtration of the solids followed by cake washing with 25% toluene in heptane (2.5 L, 5 L/kg) and heptane (2.5 mL, 5 L/kg) and drying under vacuum at 50 °C provided **1** as a beige crystalline solid, 485 g (99.4 LCAP purity, 73% yield).

Optimized Process. A solution of 1-(tetrahydro-2*H*-pyran-2-yl)-1*H*-pyrazole **2** (290 g, 1.9 mol, 1.3 equiv) in THF (2.4 L, 8 L/kg) was inerted via subsurface N_2 sparging and cooled to −10 °C. A solution of hexyllithium in hexane (620 g, 2.2 M, 2.7 mol, 1.4 equiv) was charged over 30 min such that the internal temperature remained below 5 °C. After aging the slurry for 20 min, a solution of $ZnCl_2$ in 2-methyltetrahydrofuran (1.0 kg, 1.9 M, 2.7 mol, 1.4 equiv) was added portionwise such that the internal temperature remained below 5 °C. The slurry was warmed to 20 °C and inerted via subsurface N_2 sparging. 5-Bromo-2-chloroaniline **3** (300 g, 1.5 mol, 1.0 equiv), dichloro[9,9-dimethyl-4,5-bis(diphenylphosphino)xanthene]palladium(II) (11 g, 15 mmol, 0.01 equiv), and THF (0.60 L, 1.6 L/kg) were charged to the reactor. The reaction mixture was heated to 50 °C for 4 h and cooled to 20 °C once the reaction was judged to be complete by HPLC analysis.

A solution of ethylene diamine (520 g, 8.7 mol, 6 equiv) in water (2.4 L, 8 L/kg) was prepared in a separate reactor and cooled to 20 °C. The reaction stream was charged to the quench reactor over 1 h. After the mixture was stirred at 20 °C for 4 h, the lower aqueous layer was removed. The organic layer was concentrated to 1.5 L (5 L/kg) followed by constant-volume distillation and solvent exchange to *i*-PrOH. The temperature was adjusted to 50 °C followed by the addition of water (1.5 L, 5 L/kg) and aging at 50 °C for 2 h to ensure seed bed formation. The final portion of water (0.90 L, 3 L/kg) was charged at 50 °C. The batch was cooled to 20 °C over 2 h and aged at this temperature for an additional 8 h. Filtration of solids followed by cake washing with 40% isopropanol in water (1.5 L, 5 L/kg) and drying under vacuum at 50 °C provided the title compound as a beige crystalline solid, 356 g (99.6 LCAP purity, 88% yield).

^{1}H NMR (500 MHz, chloroform-d) δ 7.58 (s, 1H), 7.32 (d, J = 8.2 Hz, 1H), 6.92 (s, 1H), 6.83 (dd, J = 8.2, 1.2 Hz, 1H), 6.29 (s, 1H), 5.21 (dd, J = 10.2, 2.0 Hz, 1H), 4.21−4.10 (m, 3H), 3.62−3.57 (m, 1H), 2.61−2.53 (m, 1H), 2.09−2.04 (m, 1H), 1.84 (br d, J = 12.5 Hz, 1H), 1.78−1.72 (m, 1H), 1.62−1.53 (m, 2H). ^{13}C NMR (126 MHz, chloroform-d) δ 143.4, 143.0, 139.4, 130.0, 129.5, 119.6, 119.5, 116.1, 106.4, 84.1, 67.7, 29.7, 24.8, 22.9. HRMS (ESI+) Calculated (M + H) 278.1055, found 278.1064.

■ ASSOCIATED CONTENT

Supporting Information

The Supporting Information is available free of charge at https://pubs.acs.org/doi/10.1021/acs.oprd.0c00414.

Additional HTE screening data, NMR characterization of **1**, reaction calorimetry data (PDF)

■ AUTHOR INFORMATION

Corresponding Author

Candice L. Joe − *Chemical Process Development, Bristol Myers Squibb, New Brunswick, New Jersey 08903, United States;* orcid.org/0000-0002-7167-2416; Email: Candice.joe@bms.com

Authors

Bahar Inankur − *Chemical Process Development, Bristol Myers Squibb, New Brunswick, New Jersey 08903, United States*

James Chadwick − *Chemical Process Development, Bristol Myers Squibb, Moreton, Wirral CH46 1QW, United Kingdom;* orcid.org/0000-0003-4456-0117

Sha Lou − *Chemical Process Development, Bristol Myers Squibb, New Brunswick, New Jersey 08903, United States;* orcid.org/0000-0002-4867-4106

Jeffrey Nye − *Chemical Process Development, Bristol Myers Squibb, New Brunswick, New Jersey 08903, United States*

Neil A. Strotman − *Chemical Process Development, Bristol Myers Squibb, New Brunswick, New Jersey 08903, United States;* orcid.org/0000-0002-5350-8735

Albert J. DelMonte − *Chemical Process Development, Bristol Myers Squibb, New Brunswick, New Jersey 08903, United States;* orcid.org/0000-0003-0645-3169

Complete contact information is available at: https://pubs.acs.org/10.1021/acs.oprd.0c00414

Notes

The authors declare no competing financial interest.

■ ACKNOWLEDGMENTS

The authors would like to thank Christopher Jamison for initial proof-of-concept studies for the Negishi cross-coupling, as well as Merrill Davies for early analytical support. We thank Sharla Wood for atomic spectroscopy support and Shasha Zhang for process safety evaluations. Sergei Kolotuchin, Eric Simmons, Matthew Winston, Rebecca Green, and Ling Zhang are acknowledged for helpful discussions.

■ REFERENCES

(1) Negishi, E.; King, A. O.; Okukado, N. Selective Carbon-Carbon Bond Formation Via Transition-Metal Catalysis 0.3. Highly Selective Synthesis of Unsymmetrical Biaryls and Diarylmethanes by Nickel-Catalyzed or Palladium-Catalyzed Reaction of Aryl Derivatives and Benzylzinc Derivatives with Aryl Halides. *J. Org. Chem.* **1977**, *42*, 1821−1823.

(2) Goikhman, R.; Jacques, T. L.; Sames, D. C-H Bonds as Ubiquitous Functionality: A General Approach to Complex Arylated Pyrazoles via Sequential Regioselective C-Arylation and N-Alkylation Enabled by SEM-Group Transposition. *J. Am. Chem. Soc.* **2009**, *131*, 3042−3048.

(3) Ratio of 1- to 4-arylation and 4,5-bisarylation side products was determined based on area percent using UPLCMS analysis of the end-of-reaction stream at 220 nm. The ratios are not corrected for any relative response differences between the compounds.

(4) Ahmed, B. M.; Mezei, G. Green protection of pyrazole, thermal isomerization and deprotection of tetrahydropyranylpyrazoles, and high-yield, one-pot synthesis of 3(5)-alkylpyrazoles. *RSC Adv.* **2015**, *5*, 24081−24093.

(5) (a) Vedso, P.; Begtrup, M. Synthesis of 5-Substituted 1-Hydroxypyrazoles through Directed Lithiation of 1-(Benzyloxy)-Pyrazole. *J. Org. Chem.* **1995**, *60*, 4995−4998. (b) Gerard, A. L.; Bouillon, A.; Mahatsekake, C.; Collot, V.; Rault, S. Efficient and simple synthesis of 3-aryl-1H-pyrazoles. *Tetrahedron Lett.* **2006**, *47*, 4665−4669. (c) Gerard, A. L.; Mahatsekake, C.; Collot, V.; Rault, S. A facile synthetic route to new pyrazoloisoindolones. *Tetrahedron Lett.* **2007**, *48*, 4123−4126. (d) Despotopoulou, C.; Klier, L.; Knochel, P. Synthesis of Fully Substituted Pyrazoles via Regio- and Chemo-

selective Metalations. *Org. Lett.* **2009**, *11*, 3326−3329. (e) Roy, S.; Roy, S.; Gribble, G. W., Metalation of Pyrazoles and Indazoles. In *Topics in Heterocyclic Chemistry*; Gribble, G. W., Ed.; Springer-Verlag: Berlin Heidelberg, 2012; Vol. *29*, pp 155−260. (f) Kumpulainen, E. T. T.; Pohjakallio, A. Selective Palladium-Catalyzed Direct C-H Arylation of Unsubstituted N-Protected Pyrazoles. *Adv. Synth. Catal.* **2014**, *356*, 1555−1561. (g) Mistico, L.; Querolle, O.; Meerpoel, L.; Angibaud, P.; Durandetti, M.; Maddaluno, J. Access to Silylated Pyrazole Derivatives by Palladium-Catalyzed C-H Activation of a TMS group. *Chem. - Eur. J.* **2016**, *22*, 9687−9692.

(6) Kristensen, J.; Begtrup, M.; Vedso, P. Preparation of 5-Acyl- and 5-Aryl-substituted 1-(benzyloxy)pyrazoles via directed Ortho-lithiation/transmetalation and palladium catalyzed cross-coupling. *Synthesis* **1998**, *1998*, 1604−1608.

(7) (a) Manley, P. W.; Acemoglu, M.; Marterer, W.; Pachinger, W. Large-scale Negishi coupling as applied to the synthesis of PDE472, an inhibitor of phosphodiesterase type 4D. *Org. Process Res. Dev.* **2003**, *7*, 436−445. (b) Ragan, J. A.; Raggon, J. W.; Hill, P. D.; Jones, B. P.; McDermott, R. E.; Munchhof, M. J.; Marx, M. A.; Casavant, J. M.; Cooper, B. A.; Doty, J. L.; Lu, Y. Cross-coupling methods for the large-scale preparation of an imidazole-thienopyridine: Synthesis of [2-(3-methyl-3H-imidazol-4-yl)thieno[3,2-b]pyridin-7-yl]-(2-methyl-1H-indol-5-yl)-amine. *Org. Process Res. Dev.* **2003**, *7*, 676−683. (c) Denni-Dischert, D.; Marterer, W.; Banziger, M.; Yusuff, N.; Batt, D.; Ramsey, T.; Geng, P.; Michael, W.; Wang, R. M. B.; Taplin, F.; Versace, R.; Cesarz, D.; Perez, L. B. The synthesis of a novel inhibitor of B-Raf kinase. *Org. Process Res. Dev.* **2006**, *10*, 70−77. (d) Perez-Balado, C.; Willemsens, A.; Ormerod, D.; Aelterman, W.; Mertens, N. Development of a concise scaleable synthesis of 2-chloro-5-(pyridin-2-yl) pyrimidine via a Negishi cross-coupling. *Org. Process Res. Dev.* **2007**, *11*, 237−240. (e) Lu, B.; Li, G.; Roschangar, F.; Hossain, A.; Herter, R.; Farina, V.; Senanayake, C. H. Development of a Practical Negishi Coupling Process for the Manufacturing of BILB 1941, an HCV Polymerase Inhibitor. In *Transition Metal-Catalyzed Couplings in Process Chemistry*; Dunetz, J. M. J. R., Ed.; Wiley-VCH: Weinheim, Germany, 2013; pp 105−120. (f) Acemoglu, M.; Baenziger, M.; Marterer, W. Experiences with Negishi Couplings on Technical Scale in Early Development. In *Transition Metal-Catalyzed Couplings in Process Chemistry*; Dunetz, J., Dunetz, J. R., Eds.; Wiley-VCH: Weinheim, Germany, 2013; pp 15−23. (g) Shu, L. H.; Wang, P.; Gu, C.; Liu, W.; Alabanza, L. M.; Zhang, Y. C. An Efficient Large-Scale Synthesis of a Naphthylacetic Acid CRTH2 Receptor Antagonist. *Org. Process Res. Dev.* **2013**, *17*, 651−657. (h) Gontcharov, A.; Dunetz, J. R. Rapid Enabling of Negishi Couplings for a Pair of mGluR5 Negative Allosteric Modulators. *Org. Process Res. Dev.* **2014**, *18*, 1145−1152. (i) Remarchuk, T.; Angelaud, R.; Askin, D.; Kumar, A.; Thompson, A. S.; Cheng, H.; Reichwein, J. F.; Chen, Y. P.; St-Jean, F. Manufacture of the PI3K beta-Sparing Inhibitor Taselisib. Part 1: Early-Stage Development Routes to the Bromobenzoxazepine Core. *Org. Process Res. Dev.* **2019**, *23*, 775−782.

(8) The impact of NMP on the reactivity in the Negishi coupling was not examined.

(9) See Table S1 in the Supporting Information for additional ligand screening data with $[Pd(allyl)Cl]_2$ and $Pd(OAc)_2$.

(10) Pyrazole **2** is an oil, whereas aniline **3** is a solid. We had confidience that, under controlled crystallization conditions, we would be able to purge excess **2**.

(11) (a) Rathman, T.; Schwindeman, J. A. Preparation, Properties, and Safe Handling of Commercial Organolithiums: Alkyllithiums, Lithium sec-Organoamides, and Lithium Alkoxides. *Org. Process Res. Dev.* **2014**, *18*, 1192−1210. (b) Anderson, N. G. *Practical Process Research and Development: A Guide for Organic Chemists*; Elsevier Science: 2012.

(12) See Supporting Information for additional details.

(13) The fact that the reaction reaches full conversion with 1.4 and 0.7 equiv of $ZnCl_2$ suggests that the both ArZnCl and Ar_2Zn species exist in solution and are capable of undergoing transmetalation to Pd. We have been unable to distinguish between the two species using *in situ* spectroscopic methods.

(14) An alternative strategy of increasing the equivalents of **2** relative to the HexLi and $ZnCl_2$ charges has also been successful at suppressing the formation of hexyl-coupled impurity **6**.

(15) (a) Konigsberger, K.; Chen, G. P.; Wu, R. R.; Girgis, M. J.; Prasad, K.; Repic, O.; Blacklock, T. J. A practical synthesis of 6-[2-(2,5-dimethoxyphenyl)ethyl]-4-ethylquinazoline and the art of removing palladium from the products of Pd-catalyzed reactions. *Org. Process Res. Dev.* **2003**, *7*, 733−742. (b) Garrett, C. E.; Prasad, K. The art of meeting palladium specifications in active pharmaceutical ingredients produced by Pd-catalyzed reactions. *Adv. Synth. Catal.* **2004**, *346*, 889−900. (c) Welch, C. J.; Albaneze-Walker, J.; Leonard, W. R.; Biba, M.; DaSilva, J.; Henderson, D.; Laing, B.; Mathre, D. J.; Spencer, S.; Bu, X. D.; Wang, T. B. Adsorbent screening for metal impurity removal in pharmaceutical process research. *Org. Process Res. Dev.* **2005**, *9*, 198−205. (d) Flahive, E. J.; Ewanicki, B. L.; Sach, N. W.; O'Neill-Slawecki, S. A.; Stankovic, N. S.; Yu, S.; Guinness, S. M.; Dunn, J. Development of an effective palladium removal process for VEGF oncology candidate AG13736 and a simple, efficient screening technique for scavenger reagent identification. *Org. Process Res. Dev.* **2008**, *12*, 637−645.

(16) The boiling points of the solvent/antisolvent mixtures were determined by Dynochem modelling using UNIFAC vapor−liquid equilibra correlations.

(17) Wisniewski, S. R.; Stevens, J. M.; Yu, M.; Fraunhoffer, K. J.; Romero, E. O.; Savage, S. A. Utilizing Native Directing Groups: Synthesis of a Selective IKur Inhibitor, BMS-919373, via a Regioselective C-H Arylation. *J. Org. Chem.* **2019**, *84*, 4704−4714.

(18) It is possible for metal levels to increase in the organic phase post-workup due to a loss of organic mass to the aqueous wash.

(19) Jimenez-Gonzalez, C.; Ponder, C. S.; Broxterman, Q. B.; Manley, J. B. Using the Right Green Yardstick: Why Process Mass intensity Is Used in the Pharmaceutical Industry To Drive More Sustainable Processes. *Org. Process Res. Dev.* **2011**, *15*, 912−917.

https://dx.doi.org/10.1021/acs.oprd.0c00414
Org. Process Res. Dev. XXXX, XXX, XXX−XXX